

AD _____

Award Number: W81XWH-05-1-0258

TITLE: Multimodality CT/SPECT Evaluation of Micelle Drug Carriers for Treatment of Breast Tumors

PRINCIPAL INVESTIGATOR: Brent D. Weinberg
Jinming Gao, Ph.D.

CONTRACTING ORGANIZATION: Case Western Reserve University
Cleveland, OH 44106

REPORT DATE: July 2007

TYPE OF REPORT: Annual Summary

PREPARED FOR: U.S. Army Medical Research and Materiel Command
Fort Detrick, Maryland 21702-5012

DISTRIBUTION STATEMENT: Approved for Public Release;
Distribution Unlimited

The views, opinions and/or findings contained in this report are those of the author(s) and should not be construed as an official Department of the Army position, policy or decision unless so designated by other documentation.

REPORT DOCUMENTATION PAGE				Form Approved OMB No. 0704-0188	
Public reporting burden for this collection of information is estimated to average 1 hour per response, including the time for reviewing instructions, searching existing data sources, gathering and maintaining the data needed, and completing and reviewing this collection of information. Send comments regarding this burden estimate or any other aspect of this collection of information, including suggestions for reducing this burden to Department of Defense, Washington Headquarters Services, Directorate for Information Operations and Reports (0704-0188), 1215 Jefferson Davis Highway, Suite 1204, Arlington, VA 22202-4302. Respondents should be aware that notwithstanding any other provision of law, no person shall be subject to any penalty for failing to comply with a collection of information if it does not display a currently valid OMB control number. PLEASE DO NOT RETURN YOUR FORM TO THE ABOVE ADDRESS.					
1. REPORT DATE 01-07-2007		2. REPORT TYPE Annual Summary		3. DATES COVERED 1 Jul 2006 – 30 Jun 2007	
4. TITLE AND SUBTITLE Multimodality CT/SPECT Evaluation of Micelle Drug Carriers for Treatment of Breast Tumors				5a. CONTRACT NUMBER	
				5b. GRANT NUMBER W81XWH-05-1-0258	
				5c. PROGRAM ELEMENT NUMBER	
6. AUTHOR(S) Brent D. Weinberg Jinming Gao, Ph.D. Email: brent.weinberg@case.edu				5d. PROJECT NUMBER	
				5e. TASK NUMBER	
				5f. WORK UNIT NUMBER	
7. PERFORMING ORGANIZATION NAME(S) AND ADDRESS(ES) Case Western Reserve University Cleveland, OH 44106				8. PERFORMING ORGANIZATION REPORT NUMBER	
9. SPONSORING / MONITORING AGENCY NAME(S) AND ADDRESS(ES) U.S. Army Medical Research and Materiel Command Fort Detrick, Maryland 21702-5012				10. SPONSOR/MONITOR'S ACRONYM(S)	
				11. SPONSOR/MONITOR'S REPORT NUMBER(S)	
12. DISTRIBUTION / AVAILABILITY STATEMENT Approved for Public Release; Distribution Unlimited					
13. SUPPLEMENTARY NOTES					
14. ABSTRACT Polymer micelles are a nanoparticle drug delivery system that has the potential to improve breast tumor treatment with chemotherapy. These nanoparticles can increase the half-life of incorporated drugs, can target tumors by incorporating tumor-specific ligands, and can be tracked with imaging through the inclusion of a radiolabel. In this study, quantum dots (QD) were incorporated into PEG/PLA micelles. These micelles were then characterized using transmission electron microscopy, dynamic light scattering, and fluorescence spectrophotometry. The quantum dots were found to be successfully incorporated into micelles, where they retained their fluorescent properties. Cancer cell lines were then treated with in vitro to measure cell uptake of QD-containing micelles. Confocal microscopy demonstrated slow and continuous uptake of micelles which accumulated in the cell cytoplasm. Future studies will measure the effects of modifying these micelles through the addition of a cRGD or other targeting ligand to increase cellular uptake. Furthermore, the last step of this study will be in vivo tracking of QD micelles while monitoring antitumor efficacy with fluorescently labeled Annexin V.					
15. SUBJECT TERMS breast cancer, micelle, quantum dots, beta lapachone, passive targeting, apoptosis, annexin					
16. SECURITY CLASSIFICATION OF:			17. LIMITATION OF ABSTRACT	18. NUMBER OF PAGES	19a. NAME OF RESPONSIBLE PERSON
a. REPORT	b. ABSTRACT	c. THIS PAGE			USAMRMC
U	U	U	UU	19	19b. TELEPHONE NUMBER (include area code)

Table of Contents

Introduction	4
Body	4
Key Research Accomplishments	8
Reportable Outcomes	8
Conclusions	9
References	9
Appendices	10

Introduction

Polymer micelles are nano-sized aggregates of amphiphilic polymers that can be used as a delivery agent for breast cancer chemotherapy. Micellar drug formulations have a number of advantages over conventional chemotherapy. First, they increase the solubility of hydrophobic drugs, making them easier to administer intravenously¹. Second, they have been shown to accumulate passively in tumors because of their leaky vasculature, which is known as the enhanced permeation and retention (EPR) effect². Third, they have considerable potential for customization, in which additional functional groups can be attached to the surface and used to modulate micelle properties. Particularly, the addition of a targeting ligand can increase the specificity of drug delivery to tumors³, and the attachment of a tracking molecule, such as a radiolabel, can facilitate tracking of micelles *in vivo*⁴. Previous work by our lab has established the fabrication of poly(ethylene glycol)/poly(ϵ -caprolactone) (PEG-PCL) micelles incorporating the anti-cancer agent doxorubicin⁵. These micelles have been further modified to include a cyclic RGD (cRGD) ligand to increase binding to endothelial cells⁶ or to incorporate superparamagnetic iron oxide (SPIO), a T₂-specific MRI contrast agent to allow MRI tracking of micelles *in vivo*⁷. Recently, our lab has recently developed techniques for incorporating the novel anticancer agent, β -lapachone, into micelles which were subsequently tested in several cell lines *in vitro*⁸. The goal of this project is develop a micelle platform for breast cancer treatment that can be tracked *in vivo* while simultaneously designing a method that can be used to assess the antitumor effects.

This report describes the accomplishments that have been achieved towards this goal in the past year based on the revised statement of work which was submitted in the 2006 annual summary. First, PEG-PLA micelles encapsulating quantum dots (QD) were produced. These micelles were subsequently characterized using transmission electron microscopy (TEM), dynamic light scattering (DLS) and fluorescence spectrophotometry. Second, the uptake of these QD-containing micelles was evaluated in SLK endothelial cancer cells *in vitro*. The future of this work will include incorporating a targeting ligand, such as cRGD or folate, onto the surface of the micelles and testing the system further. This additional testing will include monitoring the uptake of non-targeted and targeted micelles in additional cell lines *in vitro* as well as *in vivo*. Ultimately, we anticipate simultaneously using *in vivo*, tumor chamber fluorescence imaging to monitor QD-labeled micelles while simultaneously using fluorescent Annexin V to monitor the antitumor effects of the micelles.

Body

In the previous year's annual report, modifications to the previously stated aims were described. In these modifications, we proposed to use quantum dots (QDs) to label the cRGD-encoded polymer micelles and intravital imaging to examine the vascular targeting efficiency of QD-loaded micelles in a tumor chamber model in athymic nude mice. Since the previous annual report, we have pursued work towards the described modified aims, as stated here:

Modified Aim 2: Developing quantum dot labeled micelles to evaluate micelle distribution and uptake.

Modified Aim 3: Obtain *in vivo* efficacy data to optimize the design of drug-loaded micelles and compare them directly to systemic chemotherapy for treating murine breast cancer.

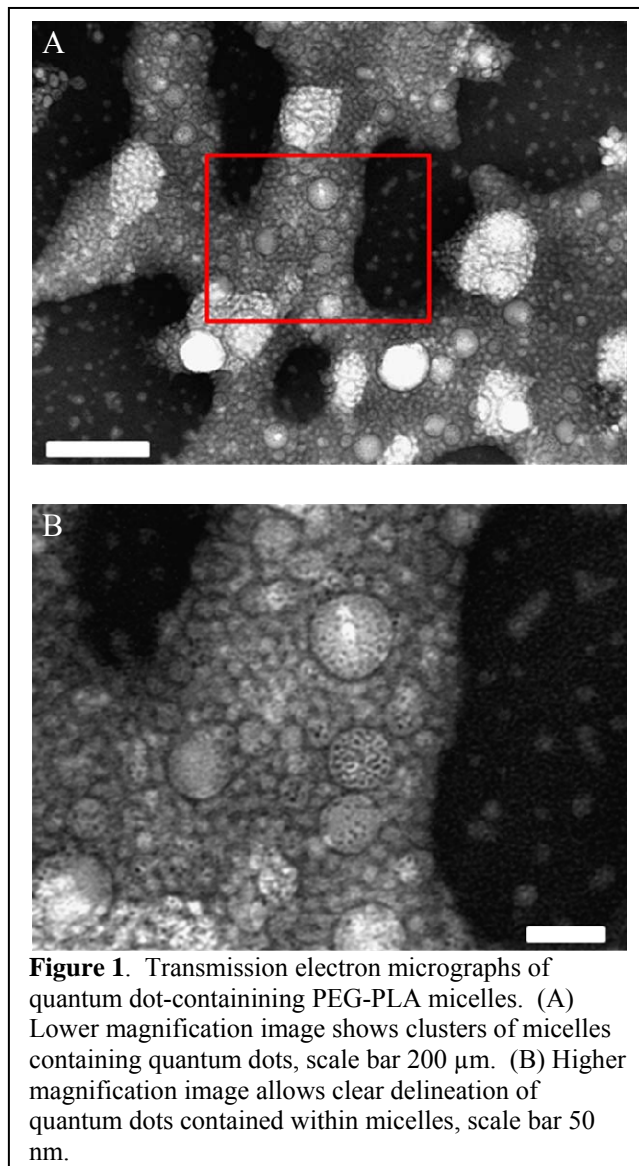
The following sections describe the progress that has been made in pursuit of each aim.

Modified Aim 2

The goal of modified aim two was to develop quantum dot labeled micelles to evaluate micelle distribution and uptake. To achieve this goal, two types of quantum dots were incorporated into polymer micelles which were subsequently characterized using transmission electron microscopy (TEM), dynamic light scattering (DLS), and fluorescence spectrophotometry. Cells were then treated with these quantum dot containing micelles *in vitro* and their intracellular uptake was measured using confocal microscopy.

Two different formulations of quantum dots were used in this study. Both formulations had a peak excitation (λ_{ex}) at approximately 350 nm; one quantum dot formulation (GCS) had a primary emission peak (λ_{em}) at 535 nm while the other micelle formulation (YCS) had a primary emission peak (λ_{em}) at 575 nm. Micelles were formulated using poly(ethylene glycol)-poly(D,L-lactide) (PEG/PLA) micelles using a solvent evaporation technique. Briefly, quantum dots and PEG/PLA were dissolved in THF. The resulting organic solution was added dropwise to water under sonication. The solution was allowed to evaporate under a hood overnight to allow for complete evaporation of THF and micelle formation.

Micelles were characterized using transmission electron microscopy (TEM), dynamic light scattering (DLS), and fluorescence spectrophotometry. Transmission electron microscopy was performed using a JEOL transmission electron microscope. Samples were negative stained with phosphotungstic acid (PTA) before imaging. Representative TEM micrographs of QD-loaded micelles are shown in Figure 1. Panel 1A shows a low magnification image showing clusters of many micelles. In the images, micelles are a lighter color than the surrounding stained space. Micelles are found to range in size from approximately 10 nm to slightly larger than 100 nm, with the majority of the micelles being in the 20 nm range. Panel 1B shows the region in the red box in higher detail. The range of micelle sizes can be seen well on this image, with some micelles as large as 50 nm but most in the range of 10-20 nm. Quantum dots can be seen within the micelles. Smaller micelles appear to contain at least 5-10 quantum dots, while larger micelles contain up to hundreds of individual quantum dots. These results indicate that micelles are formed successfully and encapsulate one or more quantum dots.



The sizes of quantum dot containing micelles were further characterized using dynamic light scattering (DLS). QD-containing micelles were diluted in water and their size measured using a Shimadzu Differential Scanning 152 Calorimeter (DSC-60, Columbia, USA). Results from DSC are seen in Figure 2A. The peak micelle size was seen at 19.0 nm, with a range of sizes from approximately 10 nm to slightly less than 100 nm. This range of sizes confirms the results which were seen on TEM and also demonstrate that there were limited numbers of large micellar aggregates in the solution.

The fluorescence of QD-containing micelles was further characterized using fluorescence spectroscopy of both unencapsulated QD and QD-containing micelles. All samples were measured on a Perkin Elmer LS-40 spectrofluorometer, with an excitation wavelength (λ_{ex}) of 350 nm. QD-only samples were diluted in THF, and QD-containing micelles were diluted in water. The results from this study are shown in Figure 2B, where the fluorescence of the QDs can be compared to the QD micelles. From this study, it appears that the fluorescence of the QDs is not markedly diminished by encapsulation in the micelles. However, the fluorescence of the QDs when encapsulated was shifted slightly toward the red end of the spectrum by several nanometers. This result could arise from several causes, such as fluorescent resonance between the closely packed quantum dots. Ultimately, these results demonstrate that quantum dots remain fluorescent when encapsulated in PEG/PLA micelles and should be viable for use in *in vitro* and *in vivo* imaging applications.

Finally, uptake of QD micelles into cells *in vitro* was measured using confocal microscopy. In this experiment, human sarcoma cells (SLK) were incubated in DMEM containing various concentrations of YCS QD-containing micelles. Polymer concentrations of the micelle solutions used were 100, 50, 25, and 0 $\mu\text{g/g}$ of media. Cells were incubated with the micelle solutions for 3 days (72 hours) and were subsequently imaged using confocal microscopy. Imaging was performed on a Nikon Eclipse confocal microscope. Excitation was performed with a laser wavelength of 404 nm, and imaging of YCS micelles was performed using a filter with a center wavelength of 600 nm and a bandwidth of 70 nm. Resulting images from the study are shown in Figure 3.

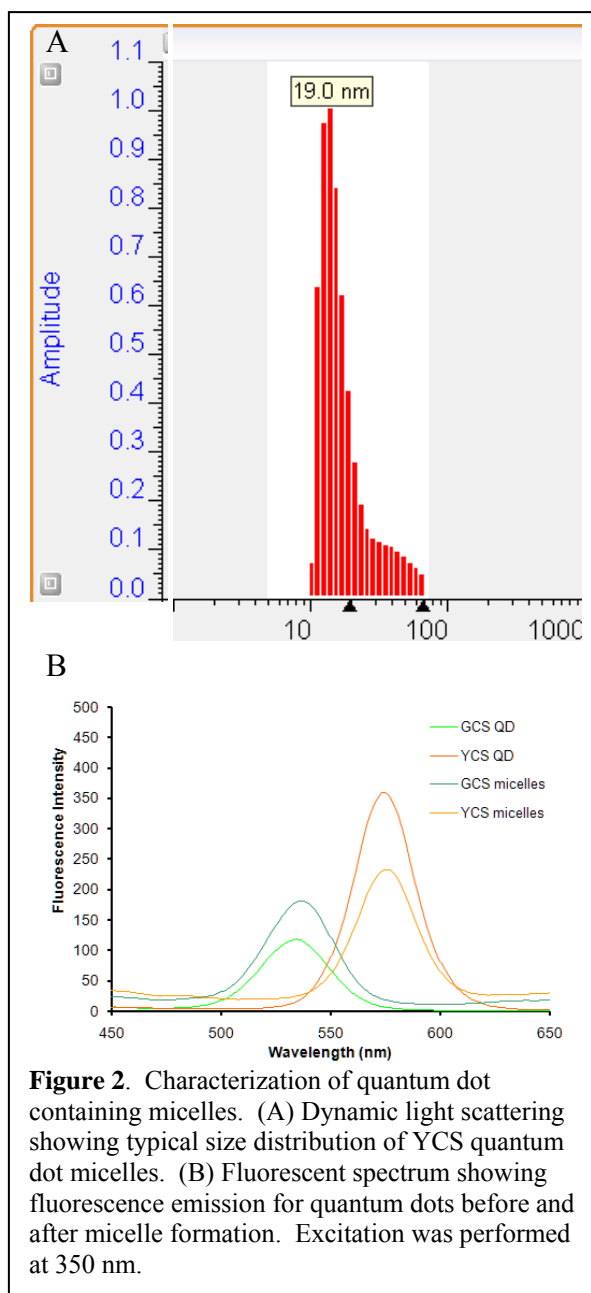
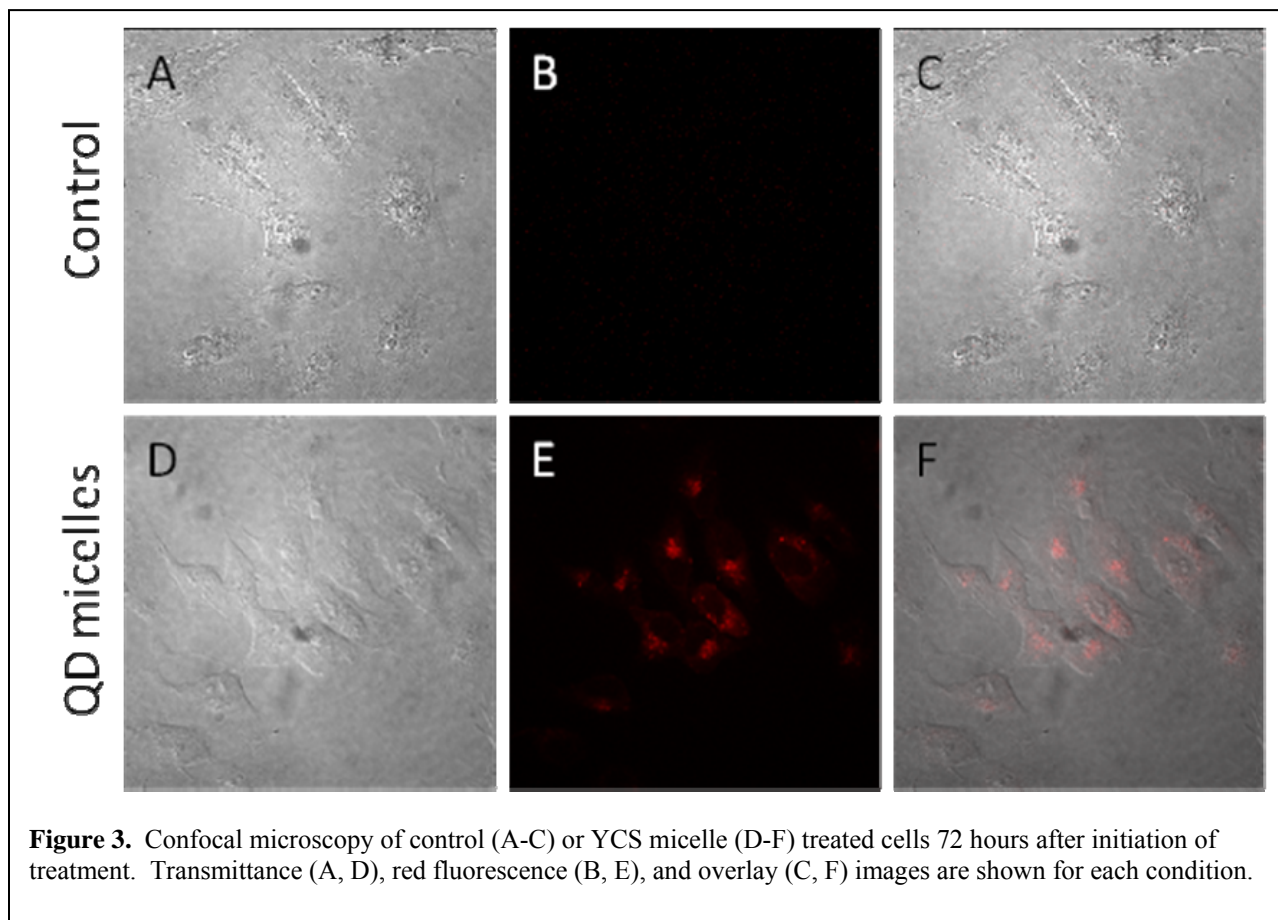


Figure 2. Characterization of quantum dot containing micelles. (A) Dynamic light scattering showing typical size distribution of YCS quantum dot micelles. (B) Fluorescent spectrum showing fluorescence emission for quantum dots before and after micelle formation. Excitation was performed at 350 nm.



In the cells treated with 0 $\mu\text{g/g}$ micelles (control), no fluorescence was seen in the cells as expected. On the other hand, cells treated with QD micelles showed considerable uptake of micelles into the cell. QD fluorescence appeared to be limited largely to the cytoplasm, a finding which has been seen often in previous studies of cell uptake of micelles. Confinement of micelle fluorescence occurs largely because the micelles only escape slowly from the cytoplasmic compartments after cell uptake. Confocal studies of cells at other time points showed that cellular uptake of the QD micelles is a steady and continuous process throughout the 72 hours (data not shown). It is anticipated that attaching a targeting ligand to the micelles as described in the aims will accelerate the uptake of micelles into the cells.

Progress towards completing modified aim 3

The results in this progress report have laid the groundwork necessary to move into the final stage of the work proposed by this grant. As described by the modified aims in last years annual report, micelles encapsulating quantum dots have been fabricated and extensively characterized. The next step will be to include the cRGD targeting ligand on the outside of the micelles to increase cell uptake. Then, rates of cell uptake can be compared *in vitro* using the targeted and non-targeted micelles in additional cell lines, including human breast cancer cell lines. Furthermore, micelles containing both QD and the anticancer agent must be fabricated. We anticipate including the anthracycline antibiotic doxorubicin, as we have in several of our previous publications. After completing this step, work will move forward into completing modified aim 3. This will include using an *in vivo* model to measure the distribution of these

QD-containing micelles *in vivo*. The model used will be a tumor chamber model of human breast cancer in athymic mice. This model will allow for *in vivo* fluorescence assessment of QD-micelle distribution as well as assessment of apoptosis *in vivo* using a fluorescent Annexin V probe. Efficacy of these treatments will then be compared to systemic chemotherapy.

Key Research Accomplishments

- Produced quantum dot (QD) loaded polymer micelles
- Characterized polymer micelles using transmission electron microscopy, dynamic light scattering, and fluorescence spectrophotometry
- Evaluated the uptake of QD-containing micelles in cultured cells *in vitro*.

Reportable Outcomes

- Refereed publications based on the project described in this grant
 - Blanco, E, EA Bey, Y Dong, BD Weinberg, DM Sutton, DA Boothman, and J Gao. β -Lapachone-containing PEG-PLA polymer micelles as novel nanotherapeutics against NQO1-overexpressing tumor cells. *J Control Release* 2007; In press. (see attached appendix)
- Other refereed publications
 - Krupka, TM, BD Weinberg, H Wu, NP Ziats, and AA Exner. Effect of Intratumoral Injection of Carboplatin Combined with Pluronic P85 or L61 on Experimental Colorectal Carcinoma in Rats. *Exp Biol Med* 2007; 232: 950-957.
 - Weinberg, BD, E Blanco, and J Gao. Polymer Implants for Intratumoral Drug Delivery and Cancer Therapy. *J Pharm Sci* 2007; In press.
 - Weinberg, BD, TM Krupka, JR Haaga, and AA Exner. A combination of sensitizing pretreatment and radiofrequency ablation evaluated in a rat carcinoma model. *Radiology* 2007; In press.
- Degrees obtained that are supported by this training grant
 - Brent Weinberg has completed the requirements for a Ph.D. in Biomedical Engineering from Case Western Reserve University. His degree will be awarded on August 10, 2007.
- Meeting abstracts and presentations
 - Weinberg, B.D., E. Blanco, S.F. Lempka, J.M. Anderson, A.A. Exner, and J. Gao. "Liver tumor treatment with combined radiofrequency ablation and doxorubicin-containing polymer implants," in *Medical Scientist Training Program Winter Retreat, Case Western Reserve University*, February 2006. Cleveland, OH.
 - Weinberg, B.D., E. Blanco, S.F. Lempka, J.M. Anderson, A.A. Exner, and J. Gao. "Liver tumor treatment with combined radiofrequency ablation and doxorubicin-containing polymer implants," in *Research Showcase, Case Western Reserve University*, April 2006. Cleveland, OH.
 - Weinberg, B.D., E. Blanco, S.F. Lempka, J.M. Anderson, A.A. Exner, and J. Gao. "Liver tumor treatment with combined radiofrequency ablation and doxorubicin-containing polymer implants," in *Lepow Research Day, Case Western Reserve University*, May 2006. Cleveland, OH.

Conclusions

In conclusion, QD-containing micelles for *in vitro* and *in vivo* tracking have been fabricated and thoroughly characterized. They have a predictable size and distribution which is favorable for use in *in vivo* studies, and incorporation of QD in a micelle core does not markedly change the fluorescence of the quantum dots. In *in vitro* cell studies, the non-targeted QD micelles were taken up at a steady rate over three days of exposure, similar to the expected outcome if these micelles were used *in vivo*. The next steps of this project should allow for the incorporation of a targeting ligand, cRGD, onto the surface of the micelle as well as including the anticancer agent, doxorubicin, in the micelle core. The result will be a multifunctional micelle which is ready to be evaluated in studies *in vivo*. For these studies, we plan to use a murine model of breast cancer in athymic mice which should allow *in vivo*, real-time assessment of fluorescent distribution to monitor the micelles. Additionally, micelle treatment efficacy will be measured using simultaneous fluorescent measurement of apoptosis. The ultimate goal of this project is to fully develop these multifunctional micelles and directly compare their efficacy to systemic chemotherapy for the treatment of a breast cancer model in mice.

References

1. Torchilin, V.P. "Targeted polymeric micelles for delivery of poorly soluble drugs." *Cell Mol Life Sci* **61**, 2549-59 (2004).
2. Matsumura, Y. and H. Maeda. "A new concept for macromolecular therapeutics in cancer chemotherapy: mechanism of tumoritropic accumulation of proteins and the antitumor agent smancs." *Cancer Res* **46**, 6387-92 (1986).
3. Otsuka, H., Y. Nagasaki, and K. Kataoka. "PEGylated nanoparticles for biological and pharmaceutical applications." *Adv Drug Deliv Rev* **55**, 403-19 (2003).
4. Sun, X., R. Rossin, J.L. Turner, M.L. Becker, M.J. Joralemon, M.J. Welch, and K.L. Wooley. "An assessment of the effects of shell cross-linked nanoparticle size, core composition, and surface PEGylation on *in vivo* biodistribution." *Biomacromolecules* **6**, 2541-54 (2005).
5. Shuai, X., H. Ai, N. Nasongkla, S. Kim, and J. Gao. "Micellar carriers based on block copolymers of poly(epsilon-caprolactone) and poly(ethylene glycol) for doxorubicin delivery." *J Control Release* **98**, 415-26 (2004).
6. Nasongkla, N., X. Shuai, H. Ai, B.D. Weinberg, J. Pink, D.A. Boothman, and J. Gao. "cRGD-functionalized polymer micelles for targeted doxorubicin delivery." *Angew Chem Int Ed Engl* **43**, 6323-7 (2004).
7. Ai, H., C. Flask, B. Weinberg, X.-T. Shuai, M.D. Pagel, D. Farrell, J. Duerk, and J. Gao. "Magnetite-Loaded Polymeric Micelles as Ultrasensitive Magnetic-Resonance Probes." *Advanced Materials* **17**, 1949-1952 (2005).
8. Blanco, E., E.A. Bey, Y. Dong, B.D. Weinberg, D.M. Sutton, D.A. Boothman, and J. Gao. "beta-Lapachone-containing PEG-PLA polymer micelles as novel nanotherapeutics against NQO1-overexpressing tumor cells." *J Control Release* In press., (2007).



β -Lapachone-containing PEG–PLA polymer micelles as novel nanotherapeutics against NQO1-overexpressing tumor cells

Elvin Blanco^a, Erik A. Bey^a, Ying Dong^a, Brent D. Weinberg^b, Damon M. Sutton^a,
David A. Boothman^a, Jinming Gao^{a,*}

^a Simmons Comprehensive Cancer Center, University of Texas Southwestern Medical Center at Dallas, Dallas, TX 75390, United States

^b Department of Biomedical Engineering, Case Western Reserve University, Cleveland, Ohio 44106, United States

Received 24 February 2007; accepted 19 April 2007

Abstract

β -Lapachone (β -lap) is a novel anticancer agent that is bioactivated by NAD(P)H: quinone oxidoreductase 1 (NQO1), an enzyme overexpressed in a variety of tumors. Despite its therapeutic promise, the poor aqueous solubility of β -lap hinders its preclinical evaluation and clinical translation. Our objective was to develop β -lap-containing poly(ethylene glycol)-block-poly(D,L-lactide) (PEG–PLA) polymer micelles for the treatment of NQO1-overexpressing tumors. Several micelle fabrication strategies were examined to maximize drug loading. A film sonication method yielded β -lap micelles with relatively high loading density ($4.7 \pm 1.0\%$ to $6.5 \pm 1.0\%$) and optimal size (29.6 ± 1.5 nm). Release studies in phosphate-buffered saline (pH 7.4) showed the time ($t_{1/2}$) for 50% of drug release at 18 h. In vitro cytotoxicity assays were performed in NQO1-overexpressing (NQO1+) and NQO1-null (NQO1–) H596 lung, DU-145 prostate, and MDA-MB-231 breast cancer cells. Cytotoxicity data showed that after a 2 h incubation with β -lap micelles, a marked increase in toxicity was shown in NQO1+ cells over NQO1– cells, resembling free drug both in efficacy and mechanism of cell death. In summary, these data demonstrate the potential of β -lap micelles as an effective therapeutic strategy against NQO1-overexpressing tumor cells.

© 2007 Published by Elsevier B.V.

Keywords: β -Lapachone; Polymer micelles; Cancer nanomedicine; Poly(ethylene glycol)–poly(D,L-lactide) (PEG–PLA); Drug delivery

1. Introduction

Presently, the development of integrated cancer nanomedicine, which consists of drugs that exploit cancer-specific molecular targets combined with effective carriers for tumor-targeted drug delivery, has shown significant promise in expanding therapeutic indices for chemotherapy. β -Lapachone (β -lap) (Fig. 1A) is a novel, plant-derived anticancer drug whose cytotoxic effect is significantly enhanced by NAD(P)H: quinone oxidoreductase 1 (NQO1), a flavoprotein found overexpressed (up to 20-fold) in a variety of human cancers, including those of the lung [1], prostate [2], pancreas [3], and breast [4]. Upon β -lap administration, NQO1 induces a futile cycling of β -lap, wherein the compound cycles between its

hydroquinone, semiquinone, and quinone forms, depleting the cell of NAD(P)H in the process and leading to the generation of DNA damaging hydroxyl radicals [5]. Additionally, β -lap treatment leads to an NQO1-dependent rise in cytosolic Ca^{2+} that results in the loss of mitochondrial membrane potential, ATP depletion, unique substrate proteolysis, DNA fragmentation, and cell apoptosis [6]. The mechanism of action is independent of caspases, p53 status, and cell cycle stage [7]. Given its central role in β -lap-mediated lethality, NQO1 is a vital, exploitable target for the treatment of cancer cells that overexpress this enzyme.

While β -lap proves to be a very promising agent from a pharmacodynamic standpoint, several factors hinder conventional intravenous administration for preclinical evaluation and clinical translation. Firstly, its non-specific distribution can lead to low tumor concentrations and systemic toxicity [8]. Moreover, its polycyclic nature makes it highly hydrophobic,

* Corresponding author. Tel.: +1 214 648 9278; fax: +1 214 648 0264.

E-mail address: jinming.gao@utsouthwestern.edu (J. Gao).

with an aqueous solubility of 0.04 mg/mL [9]. Prior work by our laboratory focused on attempts to increase the aqueous solubility of β -lap through its complexation with hydroxypropyl- β -cyclodextrin (HP β -CD) [9]. However, the fast dissociation of β -lap and cyclodextrin makes the drug susceptible to aggregation and rapid clearance, suggesting for the use of an effective nanotherapeutic delivery vehicle that can efficiently solubilize the drug and deliver it to solid tumors.

Polymer micelles are spherical, nanosized (10–100 nm) supramolecular constructs that are garnering significant attention as a versatile drug delivery platform for cancer therapy [10–12]. Polymer micelles have a unique core-shell structure as a result of the self-assembly of amphiphilic block copolymers in aqueous environments (Fig. 1B). The hydrophobic core acts as a solubilizing reservoir for water insoluble drugs, such as β -lap, providing protection from enzymatic degradation and inactivation [13]. The hydrophilic micellar corona, in turn, forms a hydrating layer on the surface of the micelle that hinders plasma protein adsorption and subsequent rapid phagocytic clearance by the reticuloendothelial system (RES) [14]. Additionally, small micellar size, along with low critical micelle concentrations (CMCs), results in long-circulating, stable constructs that do not easily dissociate in vivo [15], and contributes to the preferential accumulation of micelles in tumor tissue through the enhanced permeability and retention (EPR) effect [16,17].

To exploit these numerous advantages of polymer micelles, our objective was to develop β -lap-containing micelles for an NQO1-specific therapy. In this study, we report the development of a film sonication method to fabricate β -lap micelles with relatively high loading of the drug, adequate micelle size, core-shell formation, and favorable release characteristics. Using three different cancer cell lines, β -lap micelle treatment showed a substantial increase in cytotoxicity in NQO1+ cells over NQO1– cells, highlighting the system as a potential treatment strategy against NQO1-overexpressing tumors.

2. Materials and methods

2.1. Materials

β -lap was synthesized following a previously reported procedure [18]. PEG5k–PLA5k block copolymer (Mn = 10,000 Da) was synthesized utilizing a ring-opening polymerization procedure published previously [19]. Poly(D,L-lactide) (PLA) (Mn = 27,344 Da) was purchased from Birmingham Polymers (Pelham, AL). All organic solvents were of analytical grade. H596 non-small cell lung carcinoma (NSCLC) cells, DU-145 prostate, and MDA-MB-231 breast cancer cells, were grown in DMEM with 10% fetal bovine serum, 2 mM L-glutamine, 100 units/mL penicillin, and 100 mg/mL streptomycin at 37 °C in a humidified incubator with a 5% CO₂–95% air atmosphere. All cells were routinely found free of mycoplasma infection.

2.2. β -Lap micelle fabrication

Three distinct micelle preparation methods (dialysis, solvent evaporation, film sonication) were used to encapsulate β -lap

within PEG–PLA micelles. For all preparation methods a 10% theoretical loading (e.g. 1 mg of β -lap and 9 mg of PEG–PLA diblock copolymer) was used unless otherwise stated. In the dialysis method, the drug and polymer were dissolved in acetone, placed within a dialysis bag (MW cutoff = 2000 Da), and dialyzed against water overnight at 4 °C. The solvent evaporation method consisted of dissolving β -lap and PEG–PLA in acetone and adding the mixture dropwise to water under sonication by a Fisher Scientific Sonic Dismembrator 60 (Hampton, NH) with an output power of 0.010 W, after which the solvent was allowed to evaporate overnight. Finally, the film sonication procedure involved the dissolution of β -lap and PEG–PLA in acetone and evaporation of the solvent, yielding a solid film. Water was then added to the film and sonicated for 5 min. In each case, drug-loaded polymer micelles were filtered through 0.45 μ m nylon filters to remove non-encapsulated drug aggregates in solution, and all micelle preparations above were stored immediately at 4 °C to hinder premature drug release.

Drug loading was determined using a method previously established by Shuai et al. [19]. Briefly, 0.5 mL of micelle solution was centrifuged at a rotational speed of 2000 RPM for 30 min at 4 °C (Eppendorf Centrifuge 5804 R) using Amicon Ultra Centrifugal Filter Devices (MW cutoff = 100,000 Da). Absorbance of β -lap in the resulting supernatant was measured (λ_{max} = 257.2 nm, ϵ = 105 mL/(cm·mg β -lap) using a Perkin

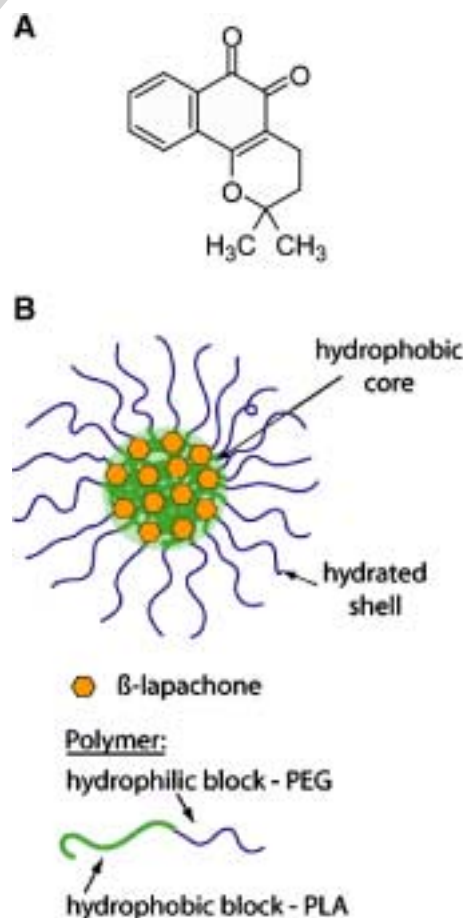


Fig. 1. (A) Chemical structure of β -lap (MW = 242 Da). (B) Schematic of a β -lap-containing polymer micelle and constituent components.

Elmer Lambda 20 UV–Vis Spectrophotometer (Fremont, CA). Micelle solutions were then lyophilized overnight and the resulting freeze-dried powder was accurately weighed, dissolved in chloroform, and analyzed via UV–Vis spectrophotometry to provide the total amount of β -lap (free and micelle encapsulated). Yield, loading efficiency, and loading density of β -lap were then determined utilizing the following set of equations:

$$\% \text{ yield} = \frac{\text{total micelle amount} - \text{free } \beta\text{-lap amount}}{\text{theoretical total micelle amount}} \times 100 \quad (1)$$

$$\% \text{ drug loading efficiency} = \frac{\text{amount } \beta\text{-lap in micelles}}{\text{initial amount of } \beta\text{-lap in system}} \times 100 \quad (2)$$

$$\% \text{ drug loading density} = \frac{\text{amount } \beta\text{-lap in micelles}}{\text{amount of micelles} - \text{free } \beta\text{-lap}} \times 100 \quad (3)$$

Micelle fabrication experiments were conducted in triplicate and following data tabulation, statistical analyses between different groups were performed using a Student's two-tailed t -test ($P < 0.05$).

2.3. Differential scanning calorimetry (DSC) analysis

DSC measurements of the solid-state solubility of β -lap in PLA were performed using a Shimadzu Differential Scanning Calorimeter (DSC-60, Columbia, USA) with samples under a nitrogen atmosphere. The procedure was adapted from a method published by Panyam et al. [20] and previously utilized by our laboratory to determine the solid-state solubility of β -lap in poly(D,L-lactide-co-glycolide) (PLGA) [21]. Briefly, known quantities of β -lap (13 mg) and PLA (27.8 mg) were separately dissolved in acetone. Different amounts of drug were mixed with polymer, and transferred to aluminum pans. The solvent was then evaporated, and pans were crimped and weighed. Samples were heated to 180 °C at a rate of 10 °C/min. The heats of melting of β -lap were obtained using the peak integration calculation method provided by the DSC software. The solid-state solubility value of β -lap was determined by plotting enthalpy values as a function of the percentage of β -lap loading. The X -intercept resulting from a linear regression of the data represents the solid-state solubility value of β -lap in PLA.

2.4. β -Lap micelle characterization

Following fabrication, micelle size was determined using a Viscotek Dynamic Light Scattering (DLS) instrument (Houston, TX). Scattered light was detected at a 90° angle. Data was obtained from 10 measurements of 5 s duration and averaged utilizing the instrumental software to determine micelle size and size distribution.

Micelles were analyzed by ^1H NMR to verify core-shell architecture. β -Lap-loaded PEG–PLA micelles were prepared

using the film sonication technique at 10% w/w theoretical drug loading. Following micelle fabrication and filtration, the micelle solution was split among two Amicon Ultra Centrifugal Filter Devices (MW cutoff=100,000 Da) and concentrated by centrifugation at a speed of 2000 RPM at 4 °C to minimize premature drug loss. Micelles were then washed with water to remove free drug. Once the absorbance of both supernatants was well below a value of 0.1, micelles were freeze-dried. One batch of micelles was resuspended in D_2O , while another batch was dissolved in deuterated chloroform. The two samples were then analyzed utilizing a 400-MHz Varian NMR spectrometer (Palo Alto, CA) and the resulting spectra were compared to spectra obtained from β -lap dissolved in D_2O and PEG–PLA dissolved in chloroform.

Release studies of β -lap-containing PEG–PLA micelles were performed to examine β -lap release kinetics. Approximately 100 mg of β -lap-loaded polymer micelles were prepared utilizing the film sonication technique at a theoretical loading of 10% w/w. After micelle fabrication, the amount of loaded drug and micelles was determined, and equal amounts of micelles were aliquoted among Spectrum Float-A-Lyzer dialysis devices with a molecular weight cutoff of 100,000 Da. Release studies were conducted in triplicate in PBS at a pH of 7.4 at 37 °C. At predetermined times, the buffer solution (12 mL) was removed and replaced with an equal amount of fresh buffer solution. The amount of β -lap released from micelles was determined by measuring the absorbance of the dialysis medium at 257.2 nm via UV–Vis spectrophotometry.

2.5. Modeling of β -lap release kinetics from micelles

Theoretical models were developed to simulate the drug release profiles from polymer micelles. Previous work has shown that drug release from a micelle core occurs in two successive stages: early release that can be well described by a Higuchi dissolution model (Eqs. (4) and (5)) and late release that is well approximated by Fickian diffusion (Eq. (6)) [22]:

$$\frac{M(t)}{M(\infty)} = 1 - \left[\left(\frac{\alpha'}{\alpha_0} \right)^3 + \frac{1}{2} \frac{c_s}{c_0} \left(\left(\frac{\alpha'}{\alpha_0} \right) + \left(\frac{\alpha'}{\alpha_0} \right)^2 - 2 \left(\frac{\alpha'}{\alpha_0} \right)^3 \right) \right] \quad (4)$$

$$c_0 (\alpha_0^3 + 2\alpha'^3 - 3\alpha_0\alpha'^2) + c_s \left(4\alpha'^2\alpha_0 + \alpha_0^3 \ln \frac{\alpha_0}{\alpha'} - \alpha_0^3 - \alpha_0^2\alpha' - 2\alpha'^3 \right) = 6Dc_s a_0 t \quad (5)$$

$$\frac{M(t)}{M(\infty)} = p \left(1 - \frac{6}{\pi^2} \exp \left(\frac{-\pi^2 D t}{a_0^2} \right) \right) \quad (6)$$

where $M(t)$ is the mass of drug released at time t and $M(\infty)$ is the amount of drug released as time approaches infinity. The Higuchi model approximates drug release as a steadily moving front of dissolving drug moving inward from the periphery of the micelle core, where the drug is contained [23]. This model

has five parameters: the radius of the micelle core, a_0 ; the distance of the moving front from the center of the core at time t , a' ; the initial micelle drug loading, c_0 ; the solubility of drug in solution, c_s ; and the diffusivity of the drug in the micelle core, D_h . Later drug release was shown to be correctly approximated by Fickian diffusion out of a sphere, which has three parameters: the fraction of the drug released at infinite time, p_0 ; the radius of the micelle core, a_0 ; and the diffusivity of drug in the micelle core, D_f [24,25]. β -Lap solubility and micelle loading were known: $c_s=0.04$ mg/mL and $c_0=8.68$ mg/mL. The radius of gyration of the 5 kD PEG corona (6.16 nm) was subtracted from the hydrodynamic micelle radius (14.6 nm) to determine the size of the micelle core, $a_0=8.44$ nm, as reported previously [22]. The drug released by 360 h was used as the drug released at infinite time, p_0 . Estimates of the two remaining unknowns, the rates of β -lap diffusion, D_h and D_f , were then calculated using non-linear least squares parameter estimation (Matlab 7.1). D_h and D_f were estimated using release data from 0–18 and 18–360 h, respectively.

2.6. Cytotoxicity of β -lap micelles in vitro

Relative survival assays based on DNA content were performed in three different cancer cell lines with isogenic expression (or inhibition of enzyme activities with dicoumarol) of NQO1 as previously described [5]. H596 non-small cell lung cancer and MDA-MB-231 breast cancer cells contain homozygous *2 NQO1 polymorphisms and thereby lack NQO1 expression. Isogenic NQO1+ counterparts were generated and characterized for β -lap free drug responses as described [5,26]. In contrast, DU-145 human prostate cancer cells endogenously over-express NQO1, and its enzyme activity can be blocked by coadministration of dicoumarol, mimicking an NQO1-deficient cell. Briefly, NQO1+ or NQO1– H596 and MDA-MB-231 cells were seeded (10,000 cells/well) into each well of 48-well plates. DU-145 cells were seeded similarly. On the following day, media were removed, and media containing predetermined doses of free β -lap drug (dissolved in DMSO) or β -lap micelles (prepared via the film sonication method) were added for a duration of 2 h. For DU-145 cells, dicoumarol at a concentration of 40 μ M was coadministered to cells to inhibit NQO1. After 2 h exposures, media were then removed, control growth media added, and cells were allowed to grow for an additional 7 days. DNA content was determined by DNA fluorescence Hoescht

dye 33258, using an adaptation of the method of Labarca and Paigen [27]. Samples were read in a Perkin Elmer HTS 7000 Bio Assay Reader (Waltham, MA) and data were expressed as means \pm SE relative growth and graphed as treated/control (T/C) values from six wells per treatment.

2.7. DNA damage and cell death assays

Distinct biological assays were conducted in NQO1+ and NQO1– H596 cells to corroborate the mechanism of action of β -lap-mediated cell death via micellar drug delivery versus responses known for free drug [7,26,28,29]. The first consisted of reactive oxygen species (ROS) analyses. Following β -lap micelle exposure to cells, ROS formation was ascertained using the conversion of non-fluorescent 5, 6-Chloromethyl-2V, 7V-dichlorodihydrofluorescein diacetate (CM-H₂DCFDA) to its fluorescent derivative (DCF) by flow cytometry (FC-500 flow cytometer, Beckman Coulter Electronics, Miami, FL) as described [30].

DNA damage analyses, or alkaline comet assays, were also performed. DNA lesions, including DNA single and double strand breaks (SSBs, DSBs, respectively), as well as DNA base damage, were assessed in single cells treated with β -lap micelles using alkaline comet assays as previously described [28,31]. Slides were stained with SYBR-green and visualized using a Nikon Eclipse TE2000-E fluorescence microscope (Melville, NY), after which digital photomicrographs were taken.

Lastly, nucleotide analyses were conducted, where changes in intracellular nicotinamide adenine dinucleotide (NAD+) levels were measured in cells after β -lap micelle exposure as described [28]. Intracellular NAD+ levels were expressed as percentage of treated divided by control (%T/C).

3. Results

3.1. Effect of different micelle fabrication methods on drug loading

Several different micelle fabrication techniques were examined with the purpose of generating β -lap micelles with an adequate size, yield, and drug loading density and efficiency. Table 1 depicts the size, yield, and loading values obtained from the three different fabrication methods. As shown in the table, from an initial 10% theoretical loading, the dialysis method produced micelles with an extremely low drug loading at $0.02 \pm 0.01\%$, as well as a poor loading efficiency ($0.08 \pm 0.04\%$) and micelle yield ($36.3 \pm 3.40\%$). The solvent evaporation procedure provided a marked improvement in β -lap loading over the dialysis method, with a loading percentage of $0.39 \pm 0.05\%$, but with a low loading efficiency of $4.12 \pm 0.64\%$. Conversely, the film sonication method produced the highest β -lap loading of micelles among all three fabrication methods, with a $4.7 \pm 1.0\%$ drug loading at a theoretical loading of 10%, a loading efficiency of $41.9 \pm 5.6\%$, and a high micelle yield of $85.3 \pm 6.7\%$. With a subsequent increase in theoretical drug loading to 20%, β -lap loading in micelles increased to $6.5 \pm 1.0\%$.

Table 1
 β -Lapachone micelle size, yield, and drug loading parameters from different fabrication procedures

Micelle fabrication method	Theoretical loading (%)	Micelle size (nm)	Yield (%)	Loading efficiency (%)	Loading density (%)
Dialysis	10	23.3 \pm 1.2	36.3 \pm 3.4	0.08 \pm 0.04	0.02 \pm 0.01
Solvent evaporation	10	17.3 \pm 0.2	95.0 \pm 1.8	4.1 \pm 0.6	0.4 \pm 0.1
Film sonication	5	28.4 \pm 2.7	88.6 \pm 3.7	39.8 \pm 1.0	2.2 \pm 0.1
	10	29.6 \pm 1.5	85.3 \pm 6.7	41.9 \pm 5.6	4.7 \pm 1.0
	20	26.8 \pm 3.2	85.2 \pm 3.0	32.9 \pm 5.9	6.5 \pm 1.0

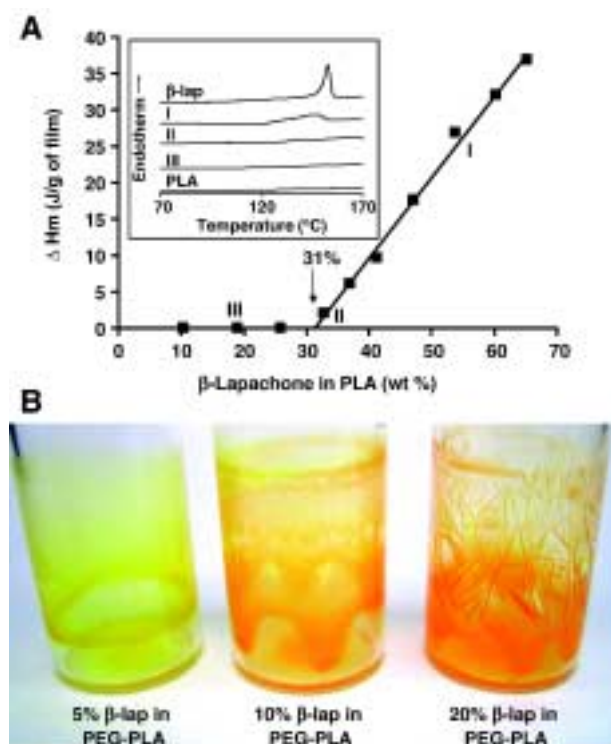


Fig. 2. Solid-state solubility studies of β -lap in PLA polymer. Fig. 2A depicts β -lap melting enthalpy (ΔH_m) as a function of β -lap loading percentage. The X-intercept indicates the solubility limit of β -lap in PLA. Fig. 2B represents images of β -lap and PLA films at different loading percentages for qualitative comparison.

Meanwhile, a lowered loading efficiency to $32.9 \pm 5.9\%$ was observed at this composition. Taken together, these data highlight the effectiveness of the film sonication method at producing higher loaded β -lap micelles over other micelle fabrication methods, with differences in loading percentage values being statistically significant ($P < 0.05$).

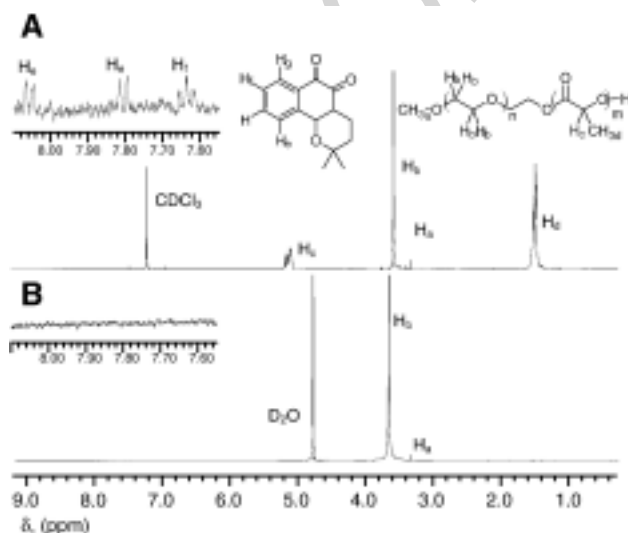


Fig. 3. ^1H NMR spectra of β -lap-loaded PEG–PLA micelles in (A) deuterated chloroform (CDCl_3) and (B) deuterated water (D_2O). Figure insets represent magnifications of the aromatic protons from β -lap.

3.2. Solubility of β -lap in PLA polymer

In order to gain insight into interactions between β -lap and the core-forming material (i.e. PLA), solid-state solubility studies were performed using DSC. Values of ΔH_m (J/g) were plotted as a function of β -lap loading percentage (Fig. 2A). The X-intercept, provided by linear regression of the data, yields the solid-state solubility of β -lap in PLA at 31%. The dissolution behavior of β -lap within PLA helps to explain discrepancies in drug loading among the different micelle fabrication procedures. Close inspection of images of β -lap/PEG5k–PLA5k films at different loading percentages illustrates the dissolution of drug within the polymer (Fig. 2B). At levels below the solid-state solubility value, the drug and polymer appear as a continuous film. However, at higher loading percentages (20%), β -lap crystals appeared in the film, indicative of drug loading above the solubility threshold of β -lap in PLA core.

3.3. β -Lap micelle characterization

Drug-loaded micelle size was determined utilizing dynamic light scattering (DLS) for each of the fabrication methods examined (Table 1). The three different methods all produced micelles of an adequate size (e.g. 10–100 nm), with the dialysis and solvent evaporation procedures yielding micelle sizes of 23.3 ± 1.2 nm and 17.3 ± 0.2 nm, respectively. The film sonication procedure produced micelles with a slightly greater average diameter (29.6 ± 1.5 nm), possibly due to the increased loading of the drug within the micelle core [32].

Encapsulation of β -lap inside micelle cores was demonstrated by comparing ^1H NMR spectra of micelle samples in deuterated chloroform (CDCl_3) and deuterated water (D_2O) (Fig. 3). In CDCl_3 , prominent resonance peaks of β -lap were observed in addition to those of PLA and PEG blocks, indicating that the micelle contains both copolymer and β -lap. In contrast, only the PEG resonance peaks were detected in D_2O , while both the PLA and β -lap resonance peaks were absent. The micelle shells consisting of PEG blocks were well solvated in D_2O and therefore showed clear ^1H NMR signal. In contrast, when β -lap was encapsulated inside micelle cores,

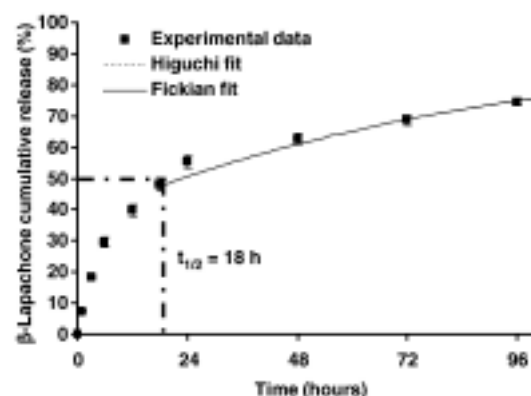


Fig. 4. In vitro β -lap release profiles from PEG–PLA polymer micelles in PBS at pH 7.4 and 37°C . The error bars were calculated as standard deviation from triplicate samples.

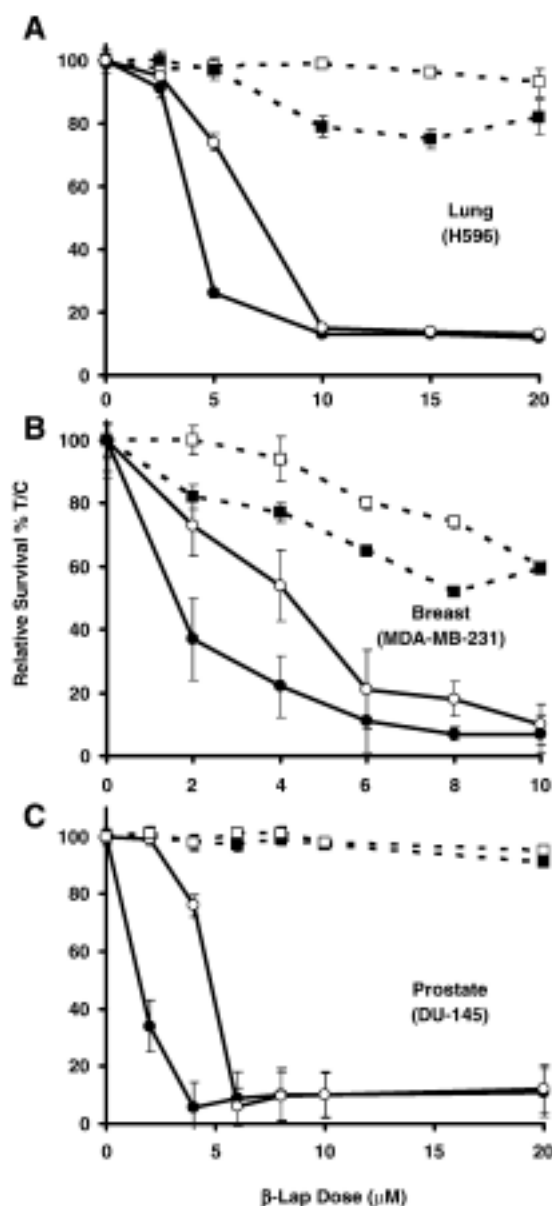


Fig. 5. Long-term, relative survival assays of (A) H596 lung, (B) DU-145 prostate, and (C) MDA-MB-231 breast cancer cells treated with β -lap at indicated doses for 2 h. In the figures, \square corresponds to NQO1 $^{-}$ cells treated with β -lap micelles, \blacksquare represents NQO1 $^{-}$ cells treated with free β -lap, \circ corresponds to NQO1 $^{+}$ cells treated with β -lap micelles, and \bullet represents NQO1 $^{+}$ cells treated with free drug.

resonance peaks of PLA blocks and β -lap were not observed due to their insufficient mobility in D_2O , consistent with the core-shell structure of polymeric micelles [33,34].

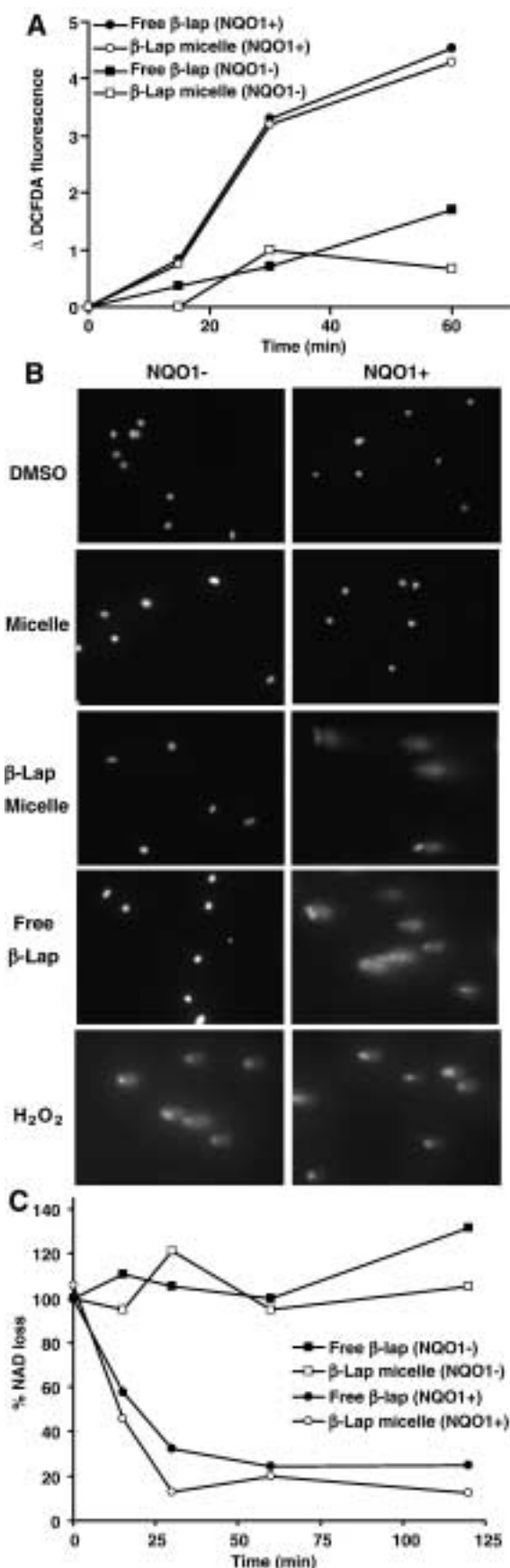
The release kinetics of β -lap from PEG-PLA polymer micelles were examined in vitro (Fig. 4). As can be seen from the figure, the time for 50% of drug release ($t_{1/2}$) is 18 h, with the majority of the drug ($\sim 75\%$) being released over the course of 4 days. Alonso and coworkers have demonstrated that PEG-PLA nanoparticles do not undergo significant degradation over two weeks incubation in PBS buffer (pH 7.4) at 37 $^{\circ}C$ [35,36]. Based on these and other findings, drug is released primarily via diffusion processes, and was modeled as such. Simulated model

drug release is shown along with experimentally measured cumulative release data. The Higuchi based model [23] output was successfully fit to the experimental measurements from 0–18 h. D_h had an estimated value of $4.2 \times 10^{-17} \text{ cm}^2/\text{s}$ (95% confidence interval: $4.0\text{--}4.4 \times 10^{-17} \text{ cm}^2/\text{s}$). After 18 h, the Fickian [24,25] diffusion approximation begins to fit the data and continues to fit the data until the end of the study. For the Fick approximation, the value of diffusion, D_f , is $2.3 \times 10^{-19} \text{ cm}^2/\text{s}$ (95% confidence interval: $2.0\text{--}2.5 \times 10^{-19} \text{ cm}^2/\text{s}$), almost 200 times slower than drug transport for the first 18 h. The quality of the model fits and low error of the parameter estimates indicate that both models well approximate the drug release data at different times of drug release. However, the diffusion rates at each stage of drug release differed considerably, suggesting that two different processes may be taking place. In the first 18 h, drug release occurs relatively quickly through a Higuchi-like mechanism. Drug released in this period of time could be precipitated in and around the micelle core but may have good access to the surrounding aqueous environment through micelle surface. However, diffusion after 18 h is dramatically slower, which may reflect drug that has less access to the surrounding hydrophilic corona. This fraction of the drug loading could be entrapped in or even dissolved in dense solid regions of the hydrophobic core, where polymer entanglement serves as a much greater impediment to drug transport.

3.4. Mechanism of action of cell death induced by β -lap micelles

Growth assays were performed to examine the mechanism of action of β -lap micelles on NQO1-overexpressing tumor cells compared to NQO1-null tumor cells. NQO1 $^{-}$ cells also serve to mimic normal tissues that are NQO1 deficient. Fig. 5 depicts relative survival curves (%T/C) in vitro of three different tumor cell lines (lung, prostate, and breast) treated with free β -lap and β -lap micelles at different drug doses. Results show that after a 2 h incubation with β -lap micelles, a significant increase in cytotoxicity can be observed in NQO1 $^{+}$ over NQO1 $^{-}$ cells in all three cell lines. In H596 cells, a 26% loss in survival in NQO1 $^{+}$ cells following 5 μM β -lap micelle administration was noted, and at 10 μM an approximate 85% loss in survival was observed. Values for β -lap micelles were consistently less cytotoxic than for free drug exposures. β -Lap micelle cytotoxicity was equal to that of free β -lap drug administration at 10 μM , with the difference in cytotoxicities at smaller doses attributed to a delay in drug release from the micelles. Finally, while free β -lap leads to an approximate 25% loss in survival in NQO1 $^{-}$ cells at a 15 μM dose, β -lap micelles have minimal toxicity in NQO1 $^{-}$ cells ($\sim 7\%$ loss in survival at 20 μM dose).

The same pattern of cell cytotoxicity for the NQO1 $^{+}$ cells and survival in the NQO1 $^{-}$ cells was evident in human prostate and breast cancer cells. In DU-145 and MDA-MB-231 cells, β -lap micelles kill more than 50% of NQO1 $^{+}$ cells at a dose of 6 μM . At further dose increases, β -lap micelle cytotoxicity approached that of free β -lap. NQO1 $^{-}$ cells were resistant to β -lap micelles. In DU-145 cells, there was less than a 10% loss in



cell survival after coadministration of dicoumarol (NQO1 inhibitor) with β -lap micelles. Similarly, NQO1- MDA-MB-231 cells were resistant to β -lap micelles. Importantly drug-free micelles were shown to have no cytotoxic effect on tumor cells (data not shown).

In attempts to elucidate whether the unique mechanism of action of β -lap was preserved through micellar delivery of the drug, several key biological assays were performed in H596 cells to identify vital components of β -lap-mediated cell death in NSCLC, as reported by Bey et al. [26]. Fig. 6 shows the results of the three biological assays (ROS analysis, comet assays, and NAD loss) conducted to examine vital characteristics of β -lap-induced cell death. Administration of β -lap micelles at a dose of 10 μ M leads to oxidative stress in NQO1+ cells in a manner identical to that of free β -lap drug administration. In contrast, β -lap-induced oxidative stress was absent in NQO1- cells. In the NQO1- cells, no DNA damage was evident after exposure with free β -lap drug or β -lap micelles. However, in the NQO1+ cells, extensive comet tail formation can be observed, indicating DNA damage. Lastly, Fig. 6C shows NAD loss associated with β -lap micelle administration to H596 cells at the 10 μ M dose. As can be observed from the figure, no NAD loss occurs in the NQO1- cells, while an exponential decrease in NAD is observed with increasing dose in micelle delivered β -lap. Taken together, these results serve to show that the unique mechanism of action of β -lap is preserved through micellar delivery.

4. Discussion

The objective of the present study was to develop polymer micelles that can effectively encapsulate β -lap with adequate loading density and minimal loss of drug and polymer. Of the three methods examined in this study, film sonication yielded micelles with the highest loading density and loading efficiency. The dialysis method has been shown to be effective in cases where the encapsulated agent is very water insoluble. Despite the low water solubility (0.04 mg/mL) of β -lap, this value is still much higher compared to agents such as paclitaxel (0.34 μ g/mL) [37]. Hence, the majority of β -lap can still be lost to the surrounding aqueous medium during dialysis, leaving only a very minimal amount ($0.02 \pm 0.01\%$) within the micelles. The solvent evaporation technique is another widely used method for micelle formation, and we have successfully formed PEG-PLA polymer micelles with high doxorubicin loading [38]. However, this method also proved inefficient at loading β -lap within micelles (loading density = $0.39 \pm 0.05\%$), mainly because of the crystallization behavior of β -lap. Both the dialysis and solvent evaporation methods have slow processes of

Fig. 6. Cell death and DNA damage assays conducted in NQO1+ and NQO1- H596 NSCLC cells at a dose of 10 μ M of free β -lap or β -lap-containing micelles. (A) Induction of ROS in H596 cells incubated for 20 min with CM-H₂DCFDA and then treated with the dose and assessed at the times indicated. (B) Alkaline comet assays of H596 following a 2 h exposure. Vehicle alone (DMSO), micelles alone, and H_2O_2 (for NQO1 independent DNA damage) served as controls. (C) Nucleotide loss following exposure and assessed at the times indicated.

micellar formation, requiring time for organic solvent to exchange with an aqueous environment or evaporate organic solvent, respectively. In contrast, β -lap crystallization is a faster kinetic process, which can result in the loss of the majority of drug to crystal formation.

The film sonication method proved effective at achieving higher drug loading density within micelles. This increased loading can be best explained by the formation of a molecular level mixture between β -lap and PLA. During the film formation process, β -lap dissolves within the PLA core at a solid-state solubility of 31% (Fig. 2A). At values below this limit, β -lap forms a homogeneous molecular-level mixture with the PLA matrix. The dissolution of drug within the polymer matrix prevents β -lap from crystallizing during micelle formation, leading to higher drug loading density within the micelles. Similar phenomenon was observed previously by Panyam et al. where an increase in drug loading correlated with increases in solid-state solubility [20]. While the film sonication method led to a significant increase in drug loading density, the loading efficiency was only approximately 40%. We hypothesize that β -lap mixed with PEG chains in the film may not be efficiently loaded inside the micelle core upon sonication. One possible strategy to overcome this limitation is to use longer core forming blocks as demonstrated by Allen et al. [39], or the addition of PLA within the film.

The film sonication method leads to micelles with an increased amount of β -lap encapsulated within the core ($4.7 \pm 1.0\%$ to $6.5 \pm 1.0\%$). Additionally, the hydrodynamic diameter of the micelles (29.6 ± 1.5 nm) as measured by DLS also proves adequate for future in vivo delivery applications. Micelles of similar diameters (e.g. SP1049C and Genexol) have shown prolonged blood circulation times [40]. ^1H NMR studies clearly demonstrated the core-shell structure of the polymer micelles produced by the film sonication procedure. The results indicate that the drug is encapsulated within the PLA micelle core and the micelle surface is stabilized with a mobile PEG corona. Such core-shell structure has the potential advantage in the protection of the drug from enzymatic degradation while the PEG layer hinders plasma protein adsorptions and particle aggregation. Gref et al. found that reduced protein adsorption depended greatly on PEG molecular weight (~ 5000 Da) and density at the surface ($\sim 2\text{--}5\%$) [41]. In a different study, Hsiue and coworkers found that PEG–PLA micelles were stable in bovine serum albumin (BSA) for incubation timepoints of up to 25 h, as evidenced by minimal change of particle size [42]. Reduction in plasma protein interaction should translate into very stable micelles following IV injection, as shown by Kataoka and coworkers, who demonstrated that 25% of injected PEG–PLA micelles were found to be stably circulating in blood vessels 24 h after injection [43]. The aforementioned Genexol[®], a paclitaxel-containing PEG–PLA micelle formulation currently in phase I clinical trials, was shown by Bang and coworkers to have a blood elimination half-life of approximately 11 h. This same study showed that the micelle formulation had significant increase in MTD, and improved antitumor efficacy when compared to a traditional paclitaxel formulation, consistent with stable drug encapsulation in micelles in vivo [44].

In vitro growth inhibition assays demonstrate that β -lap micelles effectively kill a variety of tumor cells overexpressing NQO1 while sparing NQO1[−] cells. Close examination shows that micelle-delivered β -lap is less toxic to both NQO1⁺ and NQO1[−] cells compared to the free drug (Fig. 5). Several reasons may explain this discrepancy. Firstly, the actual intracellular concentration of β -lap may be smaller in cells incubated with β -lap micelles than those with free drug. This is possible since most anticancer agents are lipophilic (as well as hydrophobic) and can easily cross cell membranes. PEG-stabilized nanoparticles are typically internalized through fluidic phase endocytosis [14], and PEG shielding can effectively reduce cell uptake, leading to a smaller drug concentration inside the cells. Secondly, after cell internalization, micelle-delivered β -lap may not be immediately available due to micelle encapsulation. In vitro drug release studies showed the value of $t_{1/2}$ is 18 h (Fig. 4). This delayed drug availability may also contribute to a lesser cytotoxicity as shown in both NQO1⁺ and NQO1[−] cells. Despite reduced in vitro toxicity, the value of β -lap micelles will likely reside in the increased drug solubility and improved pharmacokinetics over free drug during in vivo applications. In polymer–drug conjugate systems developed by Li et al. [45] and Ulbrich et al. [46] for the delivery of paclitaxel and doxorubicin respectively, the conjugated drugs showed less in vitro cytotoxicity compared to the free drugs, however, their antitumor efficacy responses were considerably higher due to increased accumulation in tumors.

Comprehensive biological studies show that the unique mechanism of action of β -lap, as shown previously by Bey et al. [26] is preserved through micellar drug delivery. In NQO1-overexpressing tumor cells incubated with β -lap micelles, reactive oxygen species (ROS) was generated (Fig. 6A) as a result of NQO1-dependent futile cycling of the β -lap and subsequent depletion of NAD(P)H from the cell (Fig. 6C). Accumulation of ROS such as hydroxyl radicals causes massive DNA damages as shown in comet assay for β -lap micelles as well as the free drug (Fig. 6B). This NQO1-specific cytotoxicity combined with micellar drug delivery bodes well for in vivo translation of the platform, where upon administration, β -lap micelles will accumulate in tumor tissue through passive targeting and release β -lap, which will only be bioactivated in the presence of high levels of NQO1. Concurrently, normal healthy tissues will be spared from the cytotoxic effect of β -lap due to lack of NQO1 expression and reduced micelle uptake.

5. Conclusions

In summary, we have successfully developed β -lap-PEG–PLA polymer micelles with adequate loading density, optimal size, core-shell structure, and diffusion-based release kinetics. Upon administration to NQO1⁺ and NQO1[−] cells, we were able to show an NQO1-dependent cytotoxicity that resembles that of free drug administration, where NQO1⁺ cells are effectively killed and NQO1[−] cells are spared. Future studies will focus on the preclinical evaluation of these micelles in NQO1-overexpressing animal tumor models.

585 Acknowledgements

586 This work was supported by an NIH grant CA90696 to JG,
 587 NIH grant CA102792 to DAB, and DOD grant W81XWH-04-
 588 1-0164 to DAB. EB is grateful for the support of a National
 589 Institutes of Health minority supplement grant. This is report
 590 CSCNP10 from the Program in Cell Stress and Cancer
 591 Nanomedicine at UT Southwestern Medical Center at Dallas.

592 References

593 [1] M. Belinsky, A.K. Jaiswal, NAD(P)H:quinone oxidoreductase1 (DT-
 594 diaphorase) expression in normal and tumor tissues, *Cancer Metastasis*
 595 *Rev.* 12 (2) (1993) 103–117.
 596 [2] C.D. Logsdon, D.M. Simeone, C. Binkley, T. Arumugam, J.K. Greenson,
 597 T.J. Giordano, D.E. Misek, R. Kuick, S. Hanash, Molecular profiling of
 598 pancreatic adenocarcinoma and chronic pancreatitis identifies multiple
 599 genes differentially regulated in pancreatic cancer, *Cancer Res.* 63 (10)
 600 (2003) 2649–2657.
 601 [3] A.M. Lewis, M. Ough, J. Du, M.S. Tsao, L.W. Oberley, J.J. Cullen,
 602 Targeting NAD(P)H:Quinone oxidoreductase (NQO1) in pancreatic
 603 cancer, *Mol. Carcinog.* (2006).
 604 [4] D. Siegel, D. Ross, Immunodetection of NAD(P)H:quinone oxidoreduc-
 605 tase 1 (NQO1) in human tissues, *Free Radic. Biol. Med.* 29 (3–4) (2000)
 606 246–253.
 607 [5] J.J. Pink, S.M. Planchon, C. Tagliarino, M.E. Varnes, D. Siegel, D.A.
 608 Boothman, NAD(P)H:Quinone oxidoreductase activity is the principal
 609 determinant of beta-lapachone cytotoxicity, *J. Biol. Chem.* 275 (8) (2000)
 610 5416–5424.
 611 [6] C. Tagliarino, J.J. Pink, G.R. Dubyak, A.L. Nieminen, D.A. Boothman,
 612 Calcium is a key signaling molecule in beta-lapachone-mediated cell
 613 death, *J. Biol. Chem.* 276 (22) (2001) 19150–19159.
 614 [7] K.E. Reinicke, E.A. Bey, M.S. Bentle, J.J. Pink, S.T. Ingalls, C.L.
 615 Hoppel, R.I. Misico, G.M. Arzac, G. Burton, W.G. Bornmann, D.
 616 Sutton, J. Gao, D.A. Boothman, Development of beta-lapachone
 617 prodrugs for therapy against human cancer cells with elevated NAD(P)
 618 H:quinone oxidoreductase 1 levels, *Clin. Cancer Res.* 11 (8) (2005)
 619 3055–3064.
 620 [8] M. Ough, A. Lewis, E.A. Bey, J. Gao, J.M. Ritchie, W. Bornmann, D.A.
 621 Boothman, L.W. Oberley, J.J. Cullen, Efficacy of beta-lapachone in
 622 pancreatic cancer treatment: exploiting the novel, therapeutic target NQO1,
 623 *Cancer Biother.* 4 (1) (2005) 95–102.
 624 [9] N. Nasongkla, A.F. Wiedmann, A. Bruening, M. Beman, D. Ray, W.G.
 625 Bornmann, D.A. Boothman, J. Gao, Enhancement of solubility and
 626 bioavailability of beta-lapachone using cyclodextrin inclusion complexes,
 627 *Pharm. Res.* 20 (10) (2003) 1626–1633.
 628 [10] G.S. Kwon, M.L. Forrest, Amphiphilic block copolymer micelles for
 629 nanoscale drug delivery, *Drug Dev. Res.* 67 (1) (2006) 15–22.
 630 [11] H. Otsuka, Y. Nagasaki, K. Kataoka, PEGylated nanoparticles for
 631 biological and pharmaceutical applications, *Adv. Drug Deliv. Rev.* 55
 632 (3) (2003) 403–419.
 633 [12] V.P. Torchilin, Micellar nanocarriers: pharmaceutical perspectives, *Pharm.*
 634 *Res.* 24 (1) (2007) 1–16.
 635 [13] M. Jones, J. Leroux, Polymeric micelles — a new generation of colloidal
 636 drug carriers, *Eur. J. Pharm. Biopharm.* 48 (2) (1999) 101–111.
 637 [14] R. Savic, L. Luo, A. Eisenberg, D. Maysinger, Micellar nanocontainers
 638 distribute to defined cytoplasmic organelles, *Science* 300 (5619) (2003)
 639 615–618.
 640 [15] V.P. Torchilin, A.N. Lukyanov, Z. Gao, B. Papahadjopoulos-Sternberg,
 641 Immunomicelles: targeted pharmaceutical carriers for poorly soluble
 642 drugs, *Proc. Natl. Acad. Sci. U. S. A.* 100 (10) (2003) 6039–6044.
 643 [16] H. Hashizume, P. Baluk, S. Morikawa, J.W. McLean, G. Thurston, S.
 644 Roberge, R.K. Jain, D.M. McDonald, Openings between defective
 645 endothelial cells explain tumor vessel leakiness, *Am. J. Pathol.* 156 (4)
 646 (2000) 1363–1380.

[17] H. Maeda, The enhanced permeability and retention (EPR) effect in tumor
 vasculature: the key role of tumor-selective macromolecular drug
 targeting, *Adv. Enzyme Regul.* 41 (2001) 189–207.
 [18] S.M. Planchon, S. Wuerzberger, B. Frydman, D.T. Witiak, P. Hutson, D.R.
 Church, G. Wilding, D.A. Boothman, Beta-lapachone-mediated apoptosis
 in human promyelocytic leukemia (HL-60) and human prostate cancer
 cells: a p53-independent response, *Cancer Res.* 55 (17) (1995) 3706–3711.
 [19] X. Shuai, H. Ai, N. Nasongkla, S. Kim, J. Gao, Micellar carriers based on
 block copolymers of poly(epsilon-caprolactone) and poly(ethylene glycol)
 for doxorubicin delivery, *J. Control. Release* 98 (3) (2004) 415–426.
 [20] J. Panyam, D. Williams, A. Dash, D. Leslie-Pelecky, V. Labhasetwar,
 Solid-state solubility influences encapsulation and release of hydrophobic
 drugs from PLGA/PLA nanoparticles, *J. Pharm. Sci.-Us* 93 (7) (2004)
 1804–1814.
 [21] F.J. Wang, E. Blanco, H. Ai, D.A. Boothman, J.M. Gao, Modulating beta-
 lapachone release from polymer millirods through cyclodextrin complex-
 ation, *J. Pharm. Sci.-Us* 95 (10) (2006) 2309–2319.
 [22] D. Sutton, S. Wang, N. Nasongkla, E. Dormidontova, J. Gao, Doxorubicin
 and beta-lapachone release and interaction with micellar core materials.
Exp. Biol. Med. Submitted for publication.
 [23] T. Higuchi, Mechanism of sustained-action medication. Theoretical
 analysis of rate of release of solid drugs dispersed in solid matrices,
J. Pharm. Sci. 52 (1963) 1145–1149.
 [24] J. Crank, *The Mathematics of Diffusion*, Oxford University Press, New
 York, NY, 1975.
 [25] P.L. Ritger, N.A. Peppas, A simple equation for description of solute
 release I. Fickian and non-fickian release from non-swellable devices in the
 form of slabs, spheres, cylinders or discs, *J. Control. Release* 5 (1) (1987)
 23–36.
 [26] E.A. Bey, M.S. Bentle, K.E. Reinicke, Y. Dong, C.R. Yang, L. Girard, J.D.
 Minna, W.G. Bornmann, J. Gao, D.A. Boothman, A novel NQO1-and
 PARP-1-mediated cell death pathway induced in non-small cell lung
 cancer cells by beta-lapachone. *Proc. Natl. Acad. Sci. U. S. A.* Submitted
 for publication.
 [27] C. Labarca, K. Paigen, A simple, rapid, and sensitive DNA assay
 procedure, *Anal. Biochem.* 102 (2) (1980) 344–352.
 [28] M.S. Bentle, K.E. Reinicke, E.A. Bey, D.R. Spitz, D.A. Boothman,
 Calcium-dependent modulation of poly(ADP-ribose) polymerase-1 alters
 cellular metabolism and DNA repair, *J. Biol. Chem.* 281 (44) (2006)
 33684–33696.
 [29] C. Tagliarino, J.J. Pink, K.E. Reinicke, S.M. Simmers, S.M. Wuerzberger-
 Davis, D.A. Boothman, Mu-calpain activation in beta-lapachone-mediated
 apoptosis, *Cancer Biother.* 2 (2) (2003) 141–152.
 [30] V. Panduri, S.A. Weitzman, N.S. Chandel, D.W. Kamp, Mitochondrial-
 derived free radicals mediate asbestos-induced alveolar epithelial cell
 apoptosis, *Am. J. Physiol., Lung Cell. Mol. Physiol.* 286 (6) (2004)
 L1220–L1227.
 [31] P.L. Olive, J.P. Banath, R.E. Durand, Heterogeneity in radiation-induced
 DNA damage and repair in tumor and normal cells measured using the
 “comet” assay, *Radiat. Res.* 122 (1) (1990) 86–94.
 [32] V.P. Torchilin, Targeted polymeric micelles for delivery of poorly soluble
 drugs, *Cell. Mol. Life Sci.* 61 (19–20) (2004) 2549–2559.
 [33] C.R. Heald, S. Stolnik, K.S. Kujawinski, C. De Matteis, M.C. Garnett, L.
 Illum, S.S. Davis, S.C. Purkiss, R.J. Barlow, P.R. Gellert, Poly(lactic
 acid)–poly(ethylene oxide) (PLA–PEG) nanoparticles: NMR studies of
 the central solidlike PLA core and the liquid PEG corona, *Langmuir* 18 (9)
 (2002) 3669–3675.
 [34] J.S. Hrkach, M.T. Peracchia, A. Domb, N. Lotan, R. Langer, Nanotech-
 nology for biomaterials engineering: structural characterization of
 amphiphilic polymeric nanoparticles by H-1 NMR spectroscopy, *Biomater-*
ials 18 (1) (1997) 27–30.
 [35] R. Gref, P. Quellec, A. Sanchez, P. Calvo, E. Dellacherie, M.J. Alonso,
 Development and characterization of CyA-loaded poly(lactic acid)–poly
 (ethylene glycol)PEG micro- and nanoparticles. Comparison with
 conventional PLA particulate carriers, *Eur. J. Pharm. Biopharm.* 51 (2)
 (2001) 111–118.
 [36] P. Quellec, R. Gref, E. Dellacherie, F. Sommer, M.D. Tran, M.J. Alonso,
 Protein encapsulation within poly(ethylene glycol)-coated nanospheres. II.

- Controlled release properties, *J. Biomed. Mater. Res.* 47 (3) (1999) 388–395.
- [37] W. Bouquet, W. Ceelen, B. Fritzinger, P. Pattyn, M. Peeters, J.P. Remon, C. Vervaet, Paclitaxel/beta-cyclodextrin complexes for hyperthermic peritoneal perfusion — formulation and stability, *Eur. J. Pharm. Biopharm.* (2006).
- [38] N. Nasongkla, E. Bey, J. Ren, H. Ai, C. Khemtong, J.S. Guthi, S.F. Chin, A.D. Sherry, D.A. Boothman, J. Gao, Multifunctional polymeric micelles as cancer-targeted, MRI-ultrasensitive drug delivery systems, *Nano Lett.* 6 (11) (2006) 2427–2430.
- [39] C. Allen, D. Maysinger, A. Eisenberg, Nano-engineering block copolymer aggregates for drug delivery, *Colloids Surf., B Biointerfaces* 16 (1–4) (1999) 3–27.
- [40] D. Sutton, N. Nasongkla, E. Blanco, J. Gao, Functionalized micellar systems for cancer targeted drug delivery. *Pharm. Res.* (In Press).
- [41] R. Gref, M. Luck, P. Quellec, M. Marchand, E. Dellacherie, S. Harnisch, T. Blunk, R.H. Muller, ‘Stealth’ corona-core nanoparticles surface modified by polyethylene glycol (PEG): influences of the corona (PEG chain length and surface density) and of the core composition on phagocytic uptake and plasma protein adsorption, *Colloids Surf., B Biointerfaces* 18 (3–4) (2000) 301–313.
- [42] C.L. Lo, C.K. Huang, K.M. Lin, G.H. Hsiue, Mixed micelles formed from graft and diblock copolymers for application in intracellular drug delivery, *Biomaterials* 28 (6) (2007) 1225–1235.
- [43] Y. Yamamoto, Y. Nagasaki, Y. Kato, Y. Sugiyama, K. Kataoka, Long-circulating poly(ethylene glycol)–poly(D,L-lactide) block copolymer micelles with modulated surface charge, *J. Control. Release* 77 (1–2) (2001) 27–38.
- [44] T.Y. Kim, D.W. Kim, J.Y. Chung, S.G. Shin, S.C. Kim, D.S. Heo, N.K. Kim, Y.J. Bang, Phase I and pharmacokinetic study of Genexol-PM, a cremophor-free, polymeric micelle-formulated paclitaxel, in patients with advanced malignancies, *Clin. Cancer Res.* 10 (11) (2004) 3708–3716.
- [45] C. Li, D.F. Yu, R.A. Newman, F. Cabral, L.C. Stephens, N. Hunter, L. Milas, S. Wallace, Complete regression of well-established tumors using a novel water-soluble poly(L-glutamic acid) paclitaxel conjugate, *Cancer Res.* 58 (11) (1998) 2404–2409.
- [46] K. Ulbrich, T. Etrych, P. Chytil, M. Jelinkova, B. Rihova, HPMACopolymers with pH-controlled release of doxorubicin — in vitro cytotoxicity and in vivo antitumor activity, *J. Control. Release* 87 (1–3) (2003) 33–47.